

# Mammalian TOR complex 2 controls the actin cytoskeleton and is rapamycin insensitive

Estela Jacinto<sup>1,3</sup>, Robbie Loewith<sup>1,3</sup>, Anja Schmidt<sup>2</sup>, Shuo Lin<sup>1</sup>, Markus A. Ruegg<sup>1</sup>, Alan Hall<sup>2</sup> and Michael N. Hall<sup>1,4</sup>

**The target of rapamycin (TOR) is a highly conserved protein kinase and a central controller of cell growth. In budding yeast, TOR is found in structurally and functionally distinct protein complexes: TORC1 and TORC2. A mammalian counterpart of TORC1 (mTORC1) has been described, but it is not known whether TORC2 is conserved in mammals. Here, we report that a mammalian counterpart of TORC2 (mTORC2) also exists. mTORC2 contains mTOR, mLST8 and mAVO3, but not raptor. Like yeast TORC2, mTORC2 is rapamycin insensitive and seems to function upstream of Rho GTPases to regulate the actin cytoskeleton. mTORC2 is not upstream of the mTORC1 effector S6K. Thus, two distinct TOR complexes constitute a primordial signalling network conserved in eukaryotic evolution to control the fundamental process of cell growth.**

In the budding yeast *Saccharomyces cerevisiae*, TOR is found in two distinct multi-protein complexes<sup>1,2</sup>. TORC1 contains LST8, KOG1 and either TOR1 or TOR2 (that is, either one of the two TOR homologues in yeast). TORC1 couples transcription, ribosome biogenesis, translation initiation, nutrient uptake and autophagy to the abundance and quality of available nutrients. Thus it functions as a temporal regulator of cell growth<sup>3</sup>. The immunosuppressive and anti-cancer drug rapamycin binds directly to TOR1 or TOR2 in TORC1 and thereby inhibits TORC1 signalling. TORC2 contains LST8, AVO1, AVO2, AVO3 and TOR2. TORC2 mediates spatial control of cell growth by polarizing the actin cytoskeleton, and thus the secretory pathway, towards the bud or growth site. TORC2 signalling is rapamycin insensitive owing to the inability of rapamycin to bind to TOR2 in TORC2 (ref. 1). Like TOR, LST8 and KOG1 have obvious sequence homologues in all eukaryotic genomes examined, and mammalian TOR (mTOR) forms a rapamycin-sensitive, TORC1-like complex with mLST8 (GβL) and raptor (mKOG1)<sup>1,4–6</sup>. Sequence homologues of the AVOs are less obvious or have been absent in earlier mammalian databases, and thus the existence of an mTORC2 has yet to be demonstrated.

Searches of more recent and complete versions of mammalian genomes revealed fragments of a probable vertebrate homologue of the TORC2-specific protein AVO3. Mammalian AVO3 (mAVO3) was cloned from mouse C2C12 cDNA and sequenced, revealing a putative

protein of 1,708 amino acids that shares about 25% identity with *S. cerevisiae* AVO3. Although there are no obvious functional domains in mAVO3, there are six regions that seem to be more highly conserved in *Saccharomyces cerevisiae*, *Dictyostelium discoideum*, *Drosophila melanogaster* and *Mus musculus* (Fig. 1a).

We wished to determine if mAVO3 shares functional similarity with yeast AVO3. Searches using BLAT (the BLAST-like alignment tool) predicted an mAVO3 transcript of about 9.5 kilobases (kb). A roughly 9.5-kb transcript was detected in all tissues examined, with a higher signal observed in skeletal muscle, kidney, placenta and leukocytes (data not shown). This tissue expression profile closely resembles that observed for the mRNAs encoding mTOR, raptor and mLST8 (refs 1,5), suggesting that mAVO3 may interact with at least some of these proteins. To test if endogenous mAVO3 forms a complex with mTOR, raptor and/or mLST8, rabbit antisera were generated that specifically recognize mAVO3 and raptor. Immunoprecipitation of mTOR from HEK293 cells co-precipitated both raptor and mAVO3 (Fig. 1b). Conversely, immunoprecipitation of either raptor or mAVO3 co-precipitated mTOR (Fig. 1b). Immunoprecipitation of mTOR, raptor or mAVO3 also co-precipitated haemagglutinin (HA)-epitope-tagged mLST8 (ref. 1; and data not shown). Importantly, immunoprecipitation of raptor did not co-precipitate mAVO3 and *vice versa*. Together, this suggests that mTOR forms two distinct complexes: one containing raptor and mLST8, and the other containing mAVO3 and mLST8. On the basis of the obvious similarity to their yeast counterparts, we refer to these two complexes as mTORC1 and mTORC2, respectively<sup>1</sup>. The integrity of mTORC2 was not altered after depletion of serum or after depletion of both serum and amino acids from the growth medium (data not shown).

We next wished to determine if mTORC2, like yeast TORC2, is insensitive to rapamycin. In yeast and mammalian cells, rapamycin binds the conserved protein FKBP12. The FKBP12–rapamycin complex subsequently binds to TOR1 or TOR2 in TORC1 (mTOR in mTORC1) and thereby inhibits TORC1 signalling. FKBP12–rapamycin fails to bind to TOR2 in yeast TORC2 and thus TORC2 signalling is insensitive to rapamycin<sup>1</sup>. To determine if FKBP12–rapamycin binds to mTORC2, an epitope-tagged version of FKBP12 was precipitated from HEK293 cells treated with drug vehicle or 200 nM rapamycin for 30 min before cell lysis. FKBP12 co-precipitated mTOR and raptor (that is, mTORC1), but

<sup>1</sup>Biozentrum, University of Basel, Klingelbergstrasse 70, CH-4056 Basel, Switzerland. <sup>2</sup>Medical Research Council Laboratory for Molecular Cell Biology, University College London, Gower Street, London WC1E 6BT, UK. <sup>3</sup>These authors contributed equally to this work.

<sup>4</sup>Correspondence should be addressed to M.N.H. (e-mail: m.hall@unibas.ch)

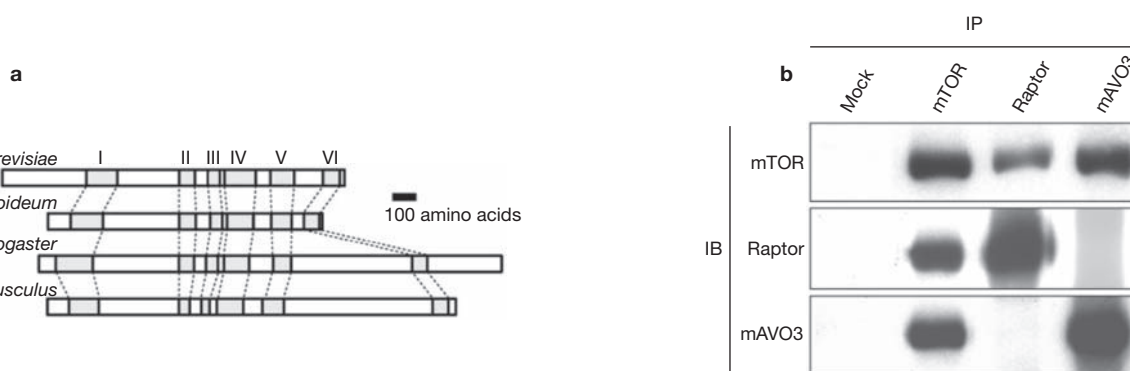


**Figure 1** mAVO3 is a functional homologue of yeast AVO3. **(a)** AVO3 orthologues from *Saccharomyces cerevisiae*, *Dictyostelium discoideum*, *Drosophila melanogaster* and *Mus musculus* were aligned using T-coffee<sup>30</sup>. Regions I–VI (In *M. musculus*, amino acids 90–215, 530–596, 645–680, 710–820, 900–990 and 1613–1678) possess the highest levels of

sequence similarity across genera. **(b)** mTOR functions in two distinct complexes. Protein extracts were prepared from sub-confluent HEK293 cells and subjected to either mock, mTOR, raptor or mAVO3 immunoprecipitation (IP). Precipitated and co-precipitated proteins were resolved on an SDS-PAGE gel and identified by immunoblotting (IB).

only from extracts of rapamycin-treated cells (Fig. 2a), indicating that the epitope-tagged FKBP12 was functional for rapamycin and mTOR binding. In contrast, FKBP12 failed to co-precipitate mAVO3 from either rapamycin-treated or rapamycin-untreated cells. The failure of FKBP12 to co-precipitate mAVO3 was not because of a rapamycin-induced dissociation of mAVO3 from mTOR, as the stability of the mAVO3–mTOR interaction was not affected by rapamycin treatment (data not shown). These observations indicate that mTORC2, like yeast TORC2, is not engaged by FKBP12–rapamycin *in vivo*.

To further investigate the rapamycin sensitivity and insensitivity of mTORC1 and mTORC2, respectively, we examined the effect of FKBP12–rapamycin treatment on mTORC1 and mTORC2 kinase activities *in vitro*. For both mTORC1 and mTORC2, autophosphorylation and phosphorylation of 4E-BP1, an *in vitro* and *in vivo* mTOR substrate<sup>7,8</sup>, were used to assay kinase activity. mTORC1 autophosphorylates mTOR, whereas mTORC2 autophosphorylates mTOR and mAVO3. mTORC1 was isolated by immunoprecipitation with anti-raptor, and mTORC2 was isolated by immunoprecipitation with anti-mAVO3. Both the mTOR autophosphorylation and the 4E-BP1 phosphorylation activities of mTORC1 were inhibited by FKBP12–rapamycin (a fivefold reduction with 200 nM rapamycin; Fig. 2b, c). In contrast, neither the mTOR and mAVO3 autophosphorylation nor the 4E-BP1 phosphorylation activities of mTORC2 were significantly affected by FKBP12–rapamycin (Fig. 2b, c). To determine if the apparent rapamycin-insensitive kinase activity of mTORC2 was indeed catalysed by mTOR, we performed kinase assays in the presence of the mTOR- and PIKK-family inhibitors LY294002 and caffeine<sup>9,10</sup>, as well as the PKA and S6K1 inhibitor H-89 (ref. 11). Raptor- and mAVO3-associated kinase activities were inhibited by 20  $\mu$ M LY294002 and 2 mM caffeine (> twofold inhibition) but not by 20  $\mu$ M H-89 (data not shown), indicating that the associated kinase activities corresponded to mTOR in mTORC1 and mTORC2, respectively. Thus, consistent with the above binding studies, mTORC1 is rapamycin sensitive, whereas mTORC2 is rapamycin insensitive.

To address if mTOR, like yeast TOR2, has a role in the control of actin cytoskeleton organization, we examined whether treatment of cells with serum, insulin or amino acids — factors known to activate mTOR signalling — affects the actin cytoskeleton. Serum-starved and amino-acid-starved NIH 3T3 fibroblasts showed few actin fibres (see Supplementary Information, Fig. S1). The addition of serum led to the rapid and robust formation of stress fibres or F-actin. This serum-induced stress-fibre formation was insensitive to prior addition of rapamycin (20 nM and

200 nM). The addition of insulin induced the formation of lamellipodia and membrane ruffles, which was also insensitive to pre-treatment with rapamycin (see Supplementary Information, Fig. S1). The addition of lysophosphatidic acid (LPA) also led to rapamycin-insensitive formation of stress fibres. Similar results were obtained with serum-, insulin- or LPA-treated Swiss 3T3 fibroblasts (data not shown). Prolonged incubation of serum-starved and amino-acid-starved NIH or Swiss 3T3 cells with amino acids (1–8 h) induced a low level of stress-fibre formation that was also rapamycin insensitive (data not shown). Thus, as shown previously for serum and insulin<sup>12</sup>, conditions that activate mTOR signalling lead to actin polymerization and cell spreading. The rapamycin insensitivity of these responses suggests that if mTOR signals to the actin cytoskeleton, it does so as part of mTORC2.

To investigate if mTORC2 indeed signals to the actin cytoskeleton, we examined the actin cytoskeleton in mTOR, mLST8, mAVO3 or raptor knock-down cells (NIH 3T3). mTOR and its partner proteins were knocked down (using small-interfering RNAs, siRNAs) in serum and nutrient-replete (unstarved) cells and in starved cells. The starved cells were re-stimulated with serum before visualization of the actin cytoskeleton. Reduced expression of target proteins in cells expressing siRNAs was confirmed, as described below. More than 80% of control cells that had been unstarved or serum re-stimulated spread into the substratum and displayed F-actin fibres (stress fibres and/or lamellipodia) (Fig. 3; also see Supplementary Information, Fig. S2). About 50% of unstarved cells and only 20% of re-stimulated cells transfected with *mTOR*, *mLST8* or *mAVO3* siRNA constructs contained F-actin and remained spread. Conversely, 90% of unstarved cells and 70% of re-stimulated cells transfected with *raptor* siRNA produced F-actin fibres and remained spread. Thus, knock-down of mTORC2, but not mTORC1, prevented actin polymerization and cell spreading, particularly in serum re-stimulated cells.

To further investigate a role for mTOR complexes in the regulation of the actin cytoskeleton, we examined paxillin phosphorylation in the mTOR, mLST8, mAVO3 or raptor knock-down cells. Paxillin is a protein that when phosphorylated localizes and recruits other signalling molecules to focal adhesions<sup>13</sup>. In control cells, paxillin was highly phosphorylated at Tyr 118 (Y118; Fig. 4a). Cells transfected with *mTOR*, *mLST8* or *mAVO3* siRNA exhibited decreased paxillin Y118 phosphorylation (Fig. 4a). Cells transfected with *raptor* siRNA displayed Y118 phosphorylation similar to that of control cells. Thus, knock-down of mTORC2, but not mTORC1, prevented paxillin phosphorylation and possibly assembly of focal adhesions. Taken together, these results

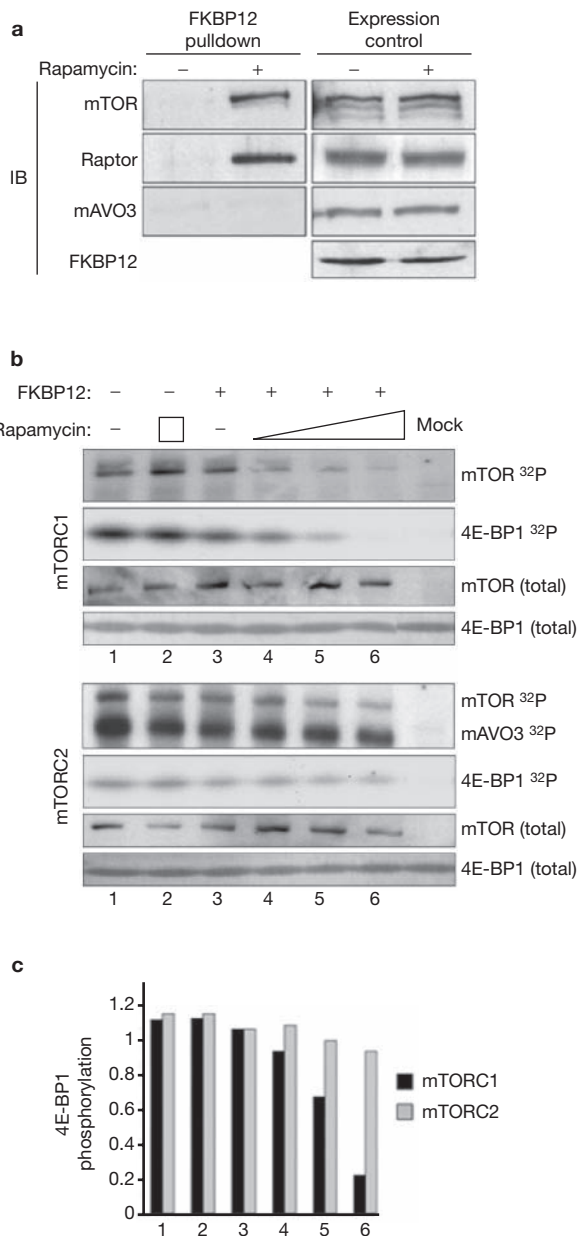


**Figure 2** mTORC2 is rapamycin insensitive. **(a)** HEK293 cells transfected with an FKBP12–TAP construct were treated with vehicle or rapamycin (200 nM) for 30 min before harvest. FKBP12–TAP was precipitated, and co-precipitated proteins (left) and protein levels in the cell lysates (right) were analysed by resolving on SDS–PAGE gels and immunoblotting. **(b)** raptor (mTORC1) and mAVO3 (mTORC2) precipitates from HEK293 cells were split equally into six tubes and re-suspended in kinase assay buffer. The following were added to the six tubes: tube 1, DMSO; tube 2, 200 nM rapamycin; tube 3, FKBP12 and DMSO; tube 4, FKBP12 and 2 nM rapamycin; tube 5, FKBP12 and 20 nM rapamycin; tube 6, FKBP12 and 200 nM rapamycin. The kinase assay using the mock immunoprecipitation contained DMSO. The autoradiographs depict mTOR and mAVO3 phosphorylation (mTOR <sup>32</sup>P and mAVO3 <sup>32</sup>P) and 4E-BP1 phosphorylation (4E-BP1 <sup>32</sup>P). Also shown are immunoblots of total mTOR protein and pictures of Coomassie-blue-stained total 4E-BP1 protein. **(c)** The log of relative phosphorylation (arbitrary unit) of 4E-BP1 by mTORC1 and mTORC2 was quantified using GeneSnap software and plotted on a graph.

suggest that mTORC2 and not mTORC1 signals to the actin cytoskeleton. Furthermore, the observation that knock-downs of mTOR, mLST8 and mAVO3 all cause a similar defect suggests that mLST8 and mAVO3 have positive roles in mTORC2 signalling.

To confirm that the siRNA constructs reduced expression of the targeted proteins (mTOR, mLST8, mAVO3 and raptor), we performed immunoblots on siRNA-transfected cells (Fig. 4a). *mTOR* and *raptor* siRNA knocked down expression of endogenous mTOR and raptor, respectively. As our anti-mLST8 and anti-mAVO3 antibodies detected endogenous mLST8 and mAVO3 in NIH 3T3 cells poorly, we co-transfected the *mLST8* and *mAVO3* siRNA constructs with vectors expressing Myc-tagged mLST8 and HA-tagged mAVO3, respectively. Expression of Myc-tagged mLST8 and HA-tagged mAVO3 was knocked down by the *mLST8* and *mAVO3* siRNA constructs. Knock-down of endogenous mAVO3 was detected in HEK293 cells (see Supplementary Information, Fig. S3a). Phosphorylation of S6K at Thr 389 was decreased in cells transfected with *mTOR*, *mLST8* or *raptor* siRNA, but not in cells transfected with *mAVO3* siRNA (Fig. 4a). Co-transfection of an excess of an HA–mTOR vector with *mTOR* siRNA restored the phosphorylation of both paxillin and S6K (Fig. 4b). Co-transfection of an excess of an HA–mLST8 or HA–raptor vector with the *mLST8* or *raptor* siRNA construct, respectively, restored S6K phosphorylation (see Supplementary Information, Fig. S3b, c). Co-transfection of an excess of an HA–mAVO3 vector with the *mAVO3* siRNA construct restored paxillin phosphorylation (see Supplementary Information, Fig. S3d). These results confirm that the siRNA constructs were functional and specific. Furthermore, they indicate that mTORC2, unlike mTORC1, does not signal to S6K, providing further evidence that the two mTOR complexes are functionally distinct.

In mammals, Rho, Rac and Cdc42 are among the well characterized members of the Rho family of GTPases that regulate F-actin assembly and disassembly<sup>14</sup>. Expression of constitutively active forms of the Rho GTPases promote organization of the actin cytoskeleton. To investigate if the mTOR and Rho or Rac pathways interact, we examined whether an active form of Rac (Rac1-L61) or Rho (RhoA-L63) restores F-actin assembly in serum re-stimulated cells that contain *mTOR*, *mLST8* or *mAVO3* siRNA. Expression of Rac1-L61 led to the formation of membrane ruffles and lamellipodia (Fig. 5a), whereas expression of RhoA-L63 induced the formation of stress fibres (see Supplementary Information, Fig. S4a) in cells co-transfected with *mTOR*, *mLST8* or *mAVO3* siRNA. Thus, activated Rac or Rho suppressed the actin defect owing to the loss of mTORC2 function, suggesting that mTORC2 may signal to the actin cytoskeleton through Rho and Rac.

To further investigate whether mTORC2 signals through a Rho-type GTPase, we examined whether mTORC2 controls the formation of active, GTP-bound Rac1. We measured, using a glutathione *S*-transferase (GST)–PAK pull-down assay, the amount of GTP-bound Rac in *mTOR*, *mLST8*, *mAVO3* or *raptor* knock-down cells. A 20–30% decrease in GTP-bound Rac1 was observed in *mTOR*-, *mLST8*- or *mAVO3*-siRNA-transfected cells relative to vector-transfected cells (Fig. 5b). In contrast, little-to-no decrease in GTP-bound Rac1 was observed in cells transfected with *raptor* siRNA. These results suggest that mTORC2 regulates Rac1 activity and thus signals through Rac1. Consistent with these findings, we observed about a twofold increase in GTP-bound Rac1 when amino acids were added to serum-starved and amino-acid-starved NIH 3T3 cells (see Supplementary Information, Fig. S4b). Addition of insulin or serum to serum-starved cells also led to a two-to-threefold increase in Rac1–GTP. Addition of amino acids or serum to starved HeLa cells stimulated GTP loading of RhoA (see Supplementary Information, Fig. S4c), consistent with the possibility that mTOR also signals through RhoA. Furthermore, the above results suggest that mTORC2, like mTORC1, responds to nutrients.

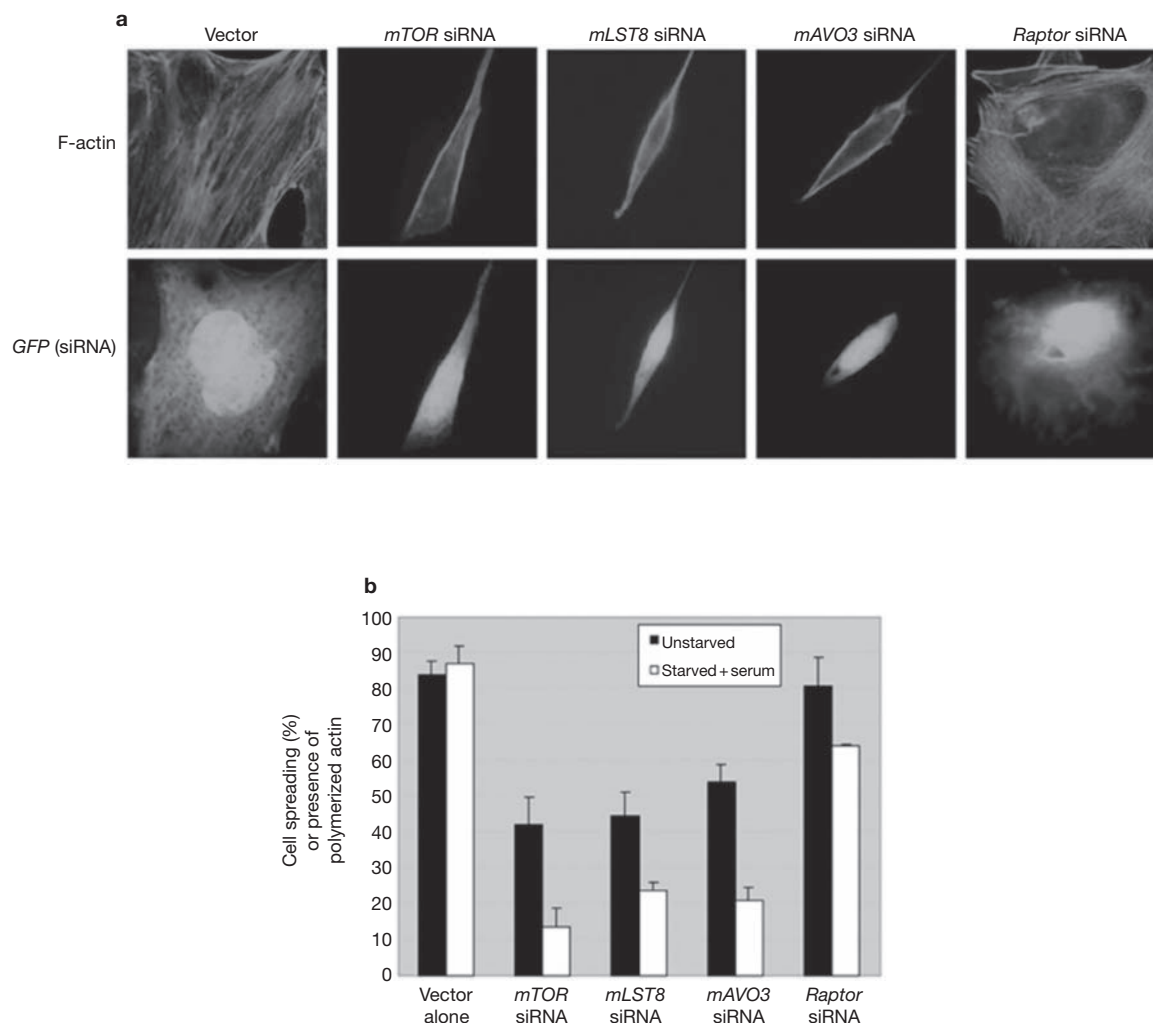


**Figure 3** mTOR, mLST8 and mAVO3, but not raptor, are involved in cell spreading and the assembly of F-actin fibres. **(a)** Transfection of siRNAs for *mTOR*, *mLST8* and *mAVO3*, but not *raptor*, inhibits cell spreading and F-actin polymerization. Transfected NIH 3T3 cells were starved of both serum (16 h) and amino acids (30 min), then re-stimulated with serum

(10×; 30 min). siRNA-transfected cells were detected by GFP fluorescence. F-actin was stained using rhodamine-phalloidin. **(b)** Quantification of transfected cells that display F-actin polymerization or spreading after the addition of serum. Results of 4–5 independent experiments were averaged and plotted. Error bars represent s.e.m.

We have described a second mTOR complex, mTORC2, that is structurally and functionally distinct from the previously identified mTORC1. mTORC2 contains mTOR, mLST8 and mAVO3, and controls the actin cytoskeleton, whereas mTORC1 contains mTOR, mLST8 and raptor, and controls protein synthesis. Furthermore, mTORC2 is rapamycin insensitive whereas mTORC1 is rapamycin sensitive. Thus, mammalian cells have two TOR complexes that are remarkably similar to the two TOR complexes previously described in yeast. TORC1 and TORC2 may constitute an ancestral signalling network conserved throughout eukaryotic evolution.

What factors are upstream of mTORC2 is not entirely clear. Growth factors, amino acids and cellular energy status signal to mTORC1 through the two tumour-suppressor proteins TSC1 and TSC2 and the GTPase Rheb<sup>7,15</sup>. Growth factors and amino acids regulate actin polymerization (see Supplementary Information, Fig. 1S)<sup>12,16</sup>, suggesting that growth factor and nutrient cues may also regulate mTORC2 through TSC and Rheb. Furthermore, TSC regulates cell adhesion<sup>17,18</sup>.

The possible factors downstream of mTORC2 are also unknown. mTORC2 seems to signal to the actin cytoskeleton through Rho GTPases. Similar to TORC2 in yeast<sup>19</sup>, mTORC2 may activate one or more Rho-type

guanine nucleotide exchange factors. Interestingly, Cdc42 and Rac1 have been implicated in the activation of S6K<sup>20,21</sup>, but this is most probably unrelated to mTORC2 signalling as mTORC2 is not required for phosphorylation of Thr 389 in S6K. 4E-BP1 could be downstream of mTORC2 as immunoprecipitated mTOR phosphorylates Thr 37 and Thr 46 in 4E-BP1, but these sites are relatively insensitive to rapamycin *in vivo*<sup>7,8</sup>. Rapamycin-insensitive mTORC2, which would be present in an mTOR immunoprecipitate, may phosphorylate these two priming sites *in vivo* allowing mTORC1 to subsequently phosphorylate the rapamycin-sensitive sites Ser 65 and Thr 70. However, contrary to this notion, mTORC2 did not phosphorylate Thr 37 and Thr 46 *in vitro* (R.L. & M.N.H., unpublished observation). mTORC2 phosphorylates 4E-BP1 *in vitro*, but at an unknown site (or sites) that may not be physiologically relevant.

The mechanism by which rapamycin inhibits mTOR activity is unclear. Given the insensitivity of mTORC2 to rapamycin, conclusions drawn from previous studies that examined the rapamycin sensitivity of immunopurified mTOR need to be re-evaluated. Previous studies, which unknowingly examined a mixture of mTORC1 and mTORC2, found that mTOR autophosphorylation, and thus intrinsic mTOR kinase activity, are rapamycin insensitive. When mTORC1 and mTORC2 were assayed



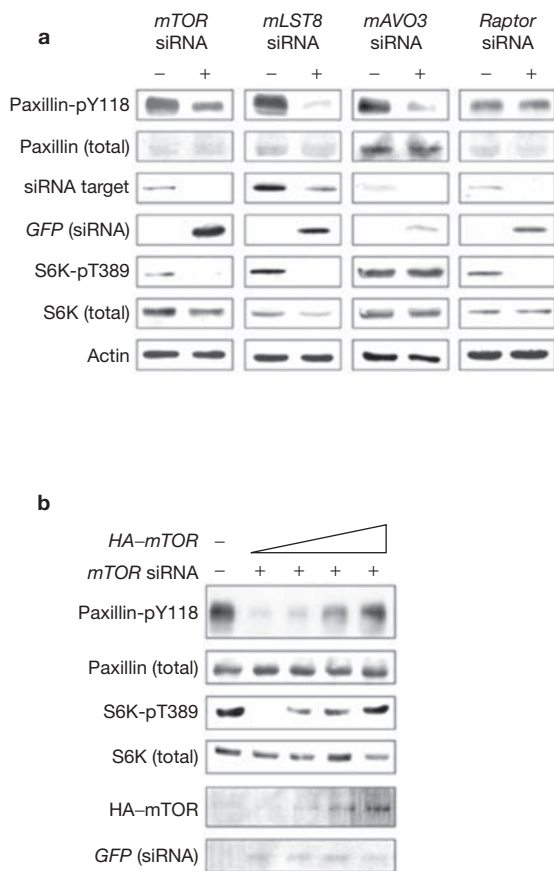


**Figure 4** mTORC1 and mTORC2 have distinct effectors. **(a)** Effect of inhibiting mTOR, mLST8, mAVO3 and raptor expression on paxillin and S6K phosphorylation. NIH 3T3 cells were transfected with 1  $\mu$ g of either pSUPER (-) or pSUPER-GFP siRNA (+) of mTOR, mLST8, mAVO3 or raptor. Cells were harvested 48 h post-transfection. Protein expression of complex members (siRNA target) was examined in total lysates. Endogenous mTOR and raptor were detected using corresponding antibodies. Myc-mLST8 or HA-mAVO3 expression constructs were cotransfected with either the *mLST8* or *mAVO3* siRNA respectively. Exogenous mLST8 or mAVO3 were detected using anti-Myc or anti-HA antibodies, respectively. **(b)** Overexpression of mTOR suppresses the effect of siRNA. pSUPER-GFP siRNA against mouse TOR (*mTOR* siRNA) was co-transfected with increasing amounts (0.1–2  $\mu$ g) of pRK5-HA-mTOR (human) in NIH 3T3 cells. Cells were harvested 48 h post-transfection.

separately, mTOR autophosphorylation by mTORC1 was rapamycin sensitive. The apparent dominance of rapamycin insensitive activity in a mixture could be because mTORC2 is more stable than mTORC1 (R.L. & M.N.H., unpublished observation). Thus, rapamycin inhibits intrinsic mTOR kinase activity (in mTORC1) rather than, or in addition to, preventing access to substrates as proposed previously<sup>22,23</sup>.

A parallel study<sup>24</sup> also identified a rapamycin-insensitive mTOR complex defined by mAVO3 (rictor). □

## METHODS

**Constructs and antibodies.** pRL41-6 is a pcDNA3-based construct (with *Bam*HI-*Xba*I sites) that expresses *M. musculus* FKBP12-1A fused to a C-terminal TAP tag. pRL68-1 is a pGEX-4T-based vector (with *Bam*HI-*Sma*I sites) that expresses *M. musculus* FKBP12-1A N-terminally fused to GST. pRL62-3 is a pCI-HA-based<sup>25</sup> construct (with *Mlu*I/*Bss*HII-*Sma*I sites) that expresses *M. musculus* mAVO3 N-terminally fused to an HA-epitope. A PCR-generated fragment of full-length mouse LST8 from IMAGE clone 4222934 was subcloned into pCI-Myc vector<sup>25</sup> at the *Eco*RI-*Xba*I sites. Myc-tagged Rac and Rho constructs were previously described<sup>26</sup>, as was PRK5-HA-mTOR<sup>27</sup>. PRK5-HA-raptor was obtained from

D. Sabatini<sup>5</sup>. For siRNA constructs, the short-hairpin RNA expression cassette, driven by the human H1 promoter<sup>28</sup> (Oligoengine, Seattle, WA), was used to subclone the annealed and ligated 64-nucleotide sequence containing the 19-nucleotide sequence from the target transcript. The 19-nucleotide sequence was designed from the following regions: mouse LST8 (bases 354–372), mouse TOR (bases 853–871), mouse raptor (bases 1,533–1,551) and mouse AVO3 (bases 2,337–2,356).

Rabbit polyclonal anti-mAVO3 antibody was raised against 6 $\times$ His-tagged, human AVO3 (amino acids 288–1,708). Rabbit polyclonal raptor antibody was generated against GST-tagged human raptor (amino acids 523–1,002). The mAVO3 and raptor fusion proteins were expressed in, and purified from, *Escherichia coli*.

**Cell culture and transfection.** HEK293 cells were maintained in DMEM containing 10% fetal bovine serum. Cells were transfected using jetPEI Reagents (Qbiogene molecular biology, Montreal, Canada) according to the manufacturer's recommendations and harvested after 24 h. Rapamycin was dissolved in DMSO (1 mg ml<sup>-1</sup>) and used at a final concentration of 200 nM.

Swiss 3T3 fibroblasts were grown on cover slips in DMEM containing 10% fetal bovine serum until confluent. To induce quiescence, cells were grown for 6–8 days without change of media. Before stimulation, cells were starved of serum overnight. Cells were also starved of nutrients the following day by resuspending cells in PBS for 1 h. Where indicated, cells were then incubated with rapamycin for 10 min, followed by the addition of amino acids and glucose, either with or without serum, or insulin. Amino acid and glucose concentrations were used at standard concentrations present in DMEM.

NIH 3T3 fibroblasts were grown on cover slips in high-glucose DMEM, with 10% fetal bovine serum (complete medium) to about 50% confluence. Cells were then transfected using Lipofectamine (Invitrogen, Carlsbad, CA), then grown for 24 h in complete medium. In unstarved conditions, cells were maintained in complete medium until harvest. For starved or re-stimulated conditions, cells were serum-starved for 16 h, then starved of amino acids for another 30 min. Unless otherwise indicated, rapamycin (20 nM) was added 10 min before stimulation. Serum stimulation was performed for 30 min.

**Immunoprecipitation of mTORC1 and mTORC2.** HEK293 cells (in 10-cm dishes; about 90% confluent) were placed on ice. Extracts from cells corresponding to half a 10-cm plate were used for each immunoprecipitation condition. Cells were washed twice with 1 ml of cold 1 $\times$  PBS and scraped in lysis buffer (0.6 ml per 10-cm plate; 40 mM HEPES, 120 mM NaCl and 0.3% CHAPS<sup>5</sup>) supplemented with protease and phosphatase inhibitors (1 $\times$  Roche complete protease inhibitor cocktail, 1 mM PMSF, 10 mM NaF, 10 mM Na<sub>3</sub>VO<sub>4</sub>, 10 mM NaPPi, 10 mM  $\beta$ -glycerophosphate, 10 mM p-nitrophenylphosphate, 0.5 mM benzamidine HCl, 1.5 mM Na<sub>3</sub>VO<sub>4</sub> and 20  $\mu$ g ml<sup>-1</sup> heparin). Crude extracts, typically 350  $\mu$ l for each immunoprecipitation, were cleared with two 3 min spins at 600g, and pre-cleared with a mixture of protein-A-, and protein-G-coupled Sepharose for 20 min. Pre-cleared lysates were subjected to immunoprecipitation with 1.5  $\mu$ l of anti-HA (for mock immunoprecipitations), anti-raptor (36T; Hall laboratory), anti-mAVO3 (15T; Hall laboratory) or 3  $\mu$ l of anti-mTOR (FRAP N19; Santa Cruz Biotechnology, Santa Cruz, CA) for 30 min at 4  $^{\circ}$ C, followed by the addition of 6  $\mu$ l of protein-A- and 6  $\mu$ l of protein-G-coupled sepharose, and incubation for an additional 90 min. In Fig. 2a, FKBP12-TAP was precipitated with 15  $\mu$ l of IgG-Sepharose beads (Amersham Biosciences, Uppsala, Sweden) for 2 h. Beads were washed three times with 1 ml of lysis buffer and resuspended in 2 $\times$  protein sample buffer or kinase assay buffer (see below).

**Kinase assays.** Kinase assays were performed in a final volume of 60  $\mu$ l containing: 40 mM HEPES, 120 mM NaCl, 0.3% CHAPS, 10 mM NaF, 10 mM Na<sub>3</sub>VO<sub>4</sub>, 10 mM  $\beta$ -glycerophosphate, 10 mM p-nitrophenylphosphate, 4 mM MnCl<sub>2</sub>, 10 mM dithiothreitol, 1 $\times$  Roche Protease inhibitor cocktail lacking EDTA, 1  $\mu$ g 4E-BP1 (Stratagene, La Jolla, CA) 80  $\mu$ M cold ATP and 10  $\mu$ M <sup>32</sup>P-ATP, and 1.67% DMSO. 500 nM GST-FKBP12 and rapamycin were added as indicated in Fig. 2b. Reactions were started with the addition of the hot and cold ATP. Tubes were maintained at 30  $^{\circ}$ C for 20 min and the reactions were terminated with the addition of 15  $\mu$ l of 5 $\times$  protein sample buffer. Proteins were then resolved on an SDS-PAGE gel. Radioactivity was detected by autoradiography, total mTOR was detected by immunoblotting and total 4E-BP1 was detected by staining with Coomassie blue.

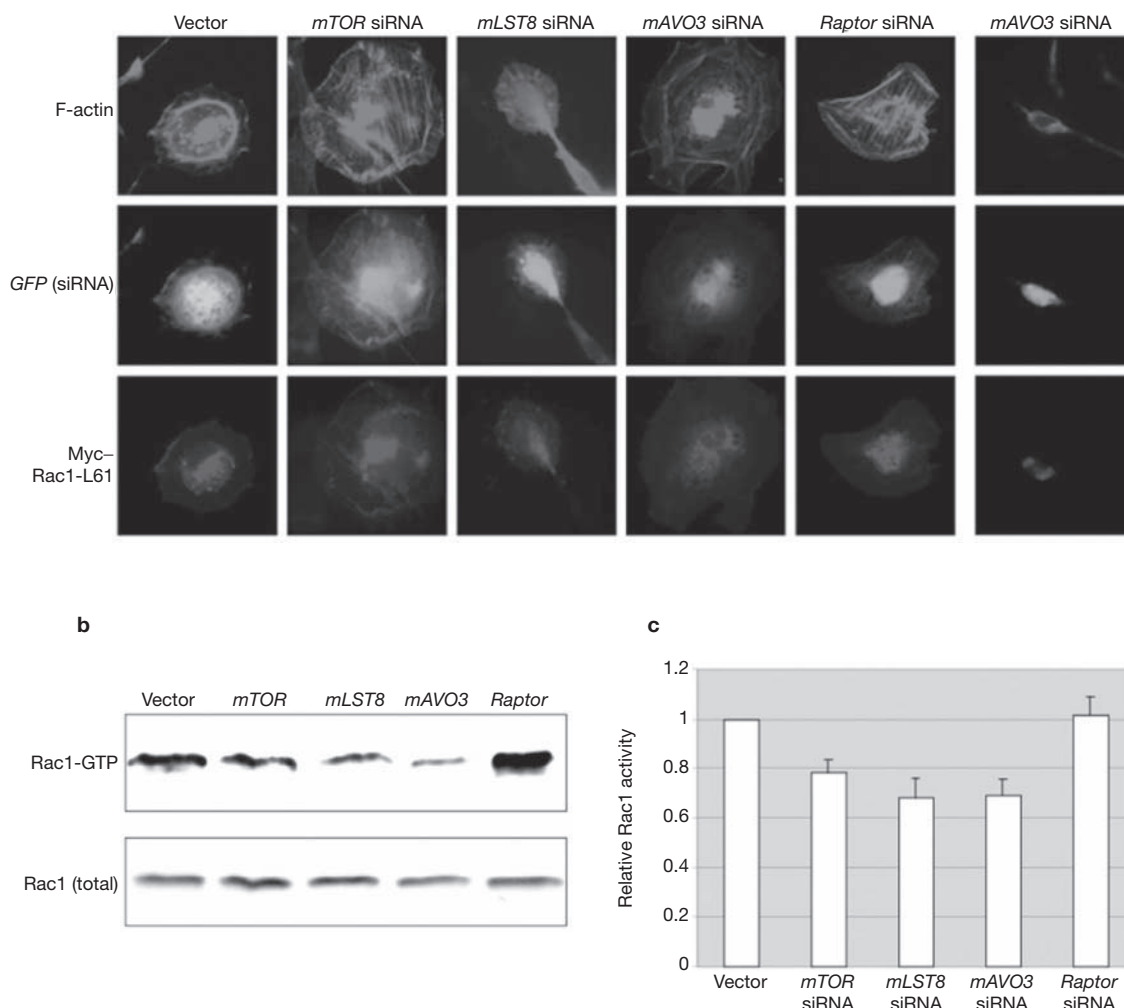


**Figure 5** mTORC2 signals through a Rho-type GTPase. **(a)** Active Rac restores membrane ruffling and lamellipodia formation in serum re-stimulated cells containing *mTOR*, *mLST8* or *mAVO3* siRNAs. NIH 3T3 cells were co-transfected with 0.5  $\mu$ g of myc-Rac1-L61 or myc plasmid (negative control; right) and 1  $\mu$ g each of the siRNA constructs. F-actin was visualized by staining cells with rhodamine-phalloidin. Cells with transfected siRNA were detected by GFP fluorescence, whereas cells co-expressing active Rac1 were visualized using an anti-Myc antibody followed by an Alexa350-conjugated anti-mouse

IgG antibody. **(b)** mTORC2 activates Rac1. NIH 3T3 cells were transfected with 10  $\mu$ g each of either vector control, *mTOR*, *mLST8*, *mAVO3* or *raptor* siRNA. Cells were harvested 48 h post-transfection. Rac1-GTP bound to GST-PAK (CRIB) beads and total cellular Rac1 was detected by immunoblotting with an anti-Rac1 antibody. A representative blot is shown. **(c)** Relative Rac1 activity was determined by comparing the amount of Rac1-GTP bound to GST-PAK (CRIB) beads compared with the total amount of cellular Rac1. Independent experiments (5–6) were averaged and plotted. Error bars represent s.e.m.

**Immunofluorescence and immunoblotting.** Cells were fixed, permeabilized and stained with rhodamine-phalloidin as described, to visualize F-actin fibres<sup>26</sup>. For localization of Myc-tagged proteins, cells were stained with mouse monoclonal anti-Myc antibody (9E10), followed by Alexa350 anti-mouse IgG (Molecular Probes, Eugene, OR). siRNA-transfected cells were visualized by GFP fluorescence and images were acquired using a Zeiss Axioplan microscope.

Immunoblots were performed using the following antibodies: mouse monoclonal antibodies (1:1,000 dilution) against Rac1 (Upstate, Charlottesville, VA), GFP (Roche), mTOR (P. Houghton), rabbit polyclonal antibodies (1:1,000 dilution) against phospho-T389 S6K, phospho-Y118 paxillin (Cell Signaling Technology, Beverly, MA), raptor (G. Thomas), total S6K (1:500; Santa Cruz Biotechnology) and total paxillin (1:500; Cell Signaling).

**Rac/Rho-GTP assay.** Sub-confluent NIH 3T3 cells or HeLa cells grown in 10-cm plastic dishes were starved and stimulated as described above. NIH 3T3 cells grown in 10-cm dishes were transfected with 10  $\mu$ g of vector or siRNA plasmid using Lipofectamine and cultured for 48 h before harvesting. Growth media was collected in 15-ml falcon tubes, to collect detached cells by centrifugation, and subsequently combined with the remaining adherent cells for lysis. Combined detached and adherent cells were washed with 5 ml of TBS, scraped and lysed

in 600  $\mu$ l of lysis buffer (50 mM Tris at pH 7.6, 1% Triton X-100, 0.5% sodium deoxycholate, 0.1% SDS, 500 mM NaCl and 50 mM MgCl<sub>2</sub>) containing protease inhibitors (1 mM PMSF, 20  $\mu$ g ml<sup>-1</sup> aprotinin, 20  $\mu$ g ml<sup>-1</sup> leupeptin and 5  $\mu$ g ml<sup>-1</sup> pepstatin). The lysate was spun for 2 min at 20,800g and at 4 °C, and the supernatant collected. An aliquot of lysate (25  $\mu$ l) was saved to check for total protein expression, whereas the rest of the lysate was used for binding with GST-PAK CRIB or GST-Rhotekin RBD beads<sup>29</sup>. Lysates with beads were rotated at 4 °C for 45 min, then spun for 2 min at 600g to collect beads. Beads were washed four times in 1 ml of wash buffer (50 mM Tris at pH 7.6, 1% Triton X-100, 500 mM NaCl and 50 mM MgCl<sub>2</sub>) containing protease inhibitors. Washed beads were then resuspended in 25 ml of SDS-PAGE sample buffer, boiled and loaded onto a 15% gel, then transferred to PVDF membranes for immunoblotting.

**BLAT searches.** BLAT searches were performed at <http://genome.ucsc.edu/>.

**Accession numbers.** *mAVO3*; accession number AY497009.

**BIND identifiers.** Nine BIND identifiers ([www.bind.ca](http://www.bind.ca)) are associated with this manuscript: 178660, 178661, 178662, 178664, 178665, 178666, 178667, 178668 and 178669.

Note: Supplementary Information is available on the Nature Cell Biology website.

# ACKNOWLEDGEMENTS

We thank A. Löschmann and W. Oppliger for technical assistance, A. Lorberg and N. Kralli for helpful discussions, R. Shioda for help with alignments and P. Houghton, G. Thomas and D. Sabatini for providing reagents. This work was supported by grants from the Cancer Research Institute (E.J.), the European Molecular Biology Organization (R.L.), Cancer Research UK (A.S. and A.H.) and the Canton of Basel and the Swiss National Science Foundation (M.N.H. and M.R.).

# COMPETING FINANCIAL INTERESTS

The authors declare that they have no competing financial interests.

Received 12 August 2004; accepted 01 September 2004

Published online at <http://www.nature.com/naturecellbiology>.

- Loewith, R. *et al.* Two TOR complexes, only one of which is rapamycin sensitive, have distinct roles in cell growth control. *Mol. Cell* **10**, 457–468 (2002).
- Wedaman, K. P. *et al.* Tor kinases are in distinct membrane-associated protein complexes in *Saccharomyces cerevisiae*. *Mol. Biol. Cell* **14**, 1204–1220 (2003).
- Jacinto, E. & Hall, M. N. Tor signalling in bugs, brain and brawn. *Nature Rev. Mol. Cell Biol.* **4**, 117–126 (2003).
- Hara, K. *et al.* Raptor, a binding partner of target of rapamycin (TOR), mediates TOR action. *Cell* **110**, 177–189 (2002).
- Kim, D. H. *et al.* mTOR interacts with raptor to form a nutrient-sensitive complex that signals to the cell growth machinery. *Cell* **110**, 163–175 (2002).
- Kim, D. H. *et al.* GβL, a positive regulator of the rapamycin-sensitive pathway required for the nutrient-sensitive interaction between raptor and mTOR. *Mol. Cell* **11**, 895–904 (2003).
- Harris, T. E. & Lawrence, J. C. TOR signaling. *Sci. STKE* **15**, 1–17 (2003).
- Gingras, A. C., Raught, B. & Sonenberg, N. mTOR signaling to translation. *Curr. Top. Microbiol. Immunol.* **279**, 169–197 (2004).
- Brunn, G. J. *et al.* Direct inhibition of the signaling functions of the mammalian target of rapamycin by the phosphoinositide 3-kinase inhibitors, wortmannin and LY294002. *EMBO J.* **15**, 5256–5267 (1996).
- Sarkaria, J. N. *et al.* Inhibition of ATM and ATR kinase activities by the radiosensitizing agent, caffeine. *Cancer Res.* **59**, 4375–4382 (1999).
- Davies, S. P., Reddy, H., Caivano, M. & Cohen, P. Specificity and mechanism of action of some commonly used protein kinase inhibitors. *Biochem. J.* **351**, 95–105 (2000).
- Ridley, A. J. Growth factor-induced actin reorganization in Swiss 3T3 cells. *Methods Enzymol.* **256**, 306–313 (1995).
- Schaller, M. D. Paxillin: a focal adhesion-associated adaptor protein. *Oncogene* **20**, 6459–6472 (2001).
- Etienne-Manneville, S. & Hall, A. Rho GTPases in cell biology. *Nature* **420**, 629–635 (2002).
- Fingar, D. C. & Blenis, J. Target of rapamycin (TOR): an integrator of nutrient and growth factor signals and coordinator of cell growth and cell cycle progression. *Oncogene* **23**, 3151–3171 (2004).
- Xia, Y. *et al.* Mammalian target of rapamycin and protein kinase A signaling mediate the cardiac transcriptional response to glutamine. *J. Biol. Chem.* **278**, 13143–13150 (2003).
- Lamb, R. F. *et al.* The TSC1 tumour suppressor hamartin regulates cell adhesion through ERM proteins and the GTPase Rho. *Nature Cell Biol.* **2**, 281–287 (2000).
- Astrinidis, A. *et al.* Tuberin, the tuberous sclerosis complex 2 tumor suppressor gene product, regulates Rho activation, cell adhesion and migration. *Oncogene* **21**, 8470–8476 (2002).
- Schmidt, A., Bickle, M., Beck, T. & Hall, M. N. The yeast phosphatidylinositol kinase homolog TOR2 activates RHO1 and RHO2 via the exchange factor ROM2. *Cell* **88**, 531–542 (1997).
- Chou, M. M. & Blenis, J. The 70 kDa S6 kinase complexes with and is activated by the Rho family G proteins Cdc42 and Rac1. *Cell* **85**, 573–583 (1996).
- Fang, Y. *et al.* PLD1 regulates mTOR signaling and mediates Cdc42 activation of S6K1. *Curr. Biol.* **13**, 2037–2044 (2003).
- Peterson, R. T., Beal, P. A., Comb, M. J. & Schreiber, S. L. FKBP12–rapamycin-associated protein (FRAP) autophosphorylates at serine 2481 under translationally repressive conditions. *J. Biol. Chem.* **275**, 7416–7423 (2000).
- Oshiro, N. *et al.* Dissociation of raptor from mTOR is a mechanism of rapamycin-induced inhibition of mTOR function. *Genes Cells* **9**, 359–366 (2004).
- Dos, D. S. *et al.* Rictor, a novel binding partner of mTOR, defines a rapamycin-insensitive and raptor-independent pathway that regulates the cytoskeleton. *Curr. Biol.* **14**, 1296–1302 (2004).
- Hubberstey, A., Yu, G., Loewith, R., Lakusta, C. & Young, D. Mammalian CAP interacts with CAP, CAP2, and actin. *J. Cell. Biochem.* **61**, 459–466 (1996).
- Ridley, A. J., Paterson, H. F., Johnston, C. L., Diekmann, D. & Hall, A. The small GTP-binding protein rac regulates growth factor-induced membrane ruffling. *Cell* **70**, 401–410 (1992).
- Dennis, P. B. *et al.* Mammalian TOR: a homeostatic ATP sensor. *Science* **294**, 1102–1105 (2001).
- Brummelkamp, T. R., Bernards, R. & Agami, R. A system for stable expression of short interfering RNAs in mammalian cells. *Science* **296**, 550–553 (2002).
- Azim, A. C., Barkalow, K. L. & Hartwig, J. H. Determination of GTP loading on Rac and Cdc42 in platelets and fibroblasts. *Methods Enzymol.* **325**, 257–263 (2000).
- Notredame, C., Higgins, D. G. & Heringa, J. T-Coffee: A novel method for fast and accurate multiple sequence alignment. *J. Mol. Biol.* **302**, 205–217 (2000).

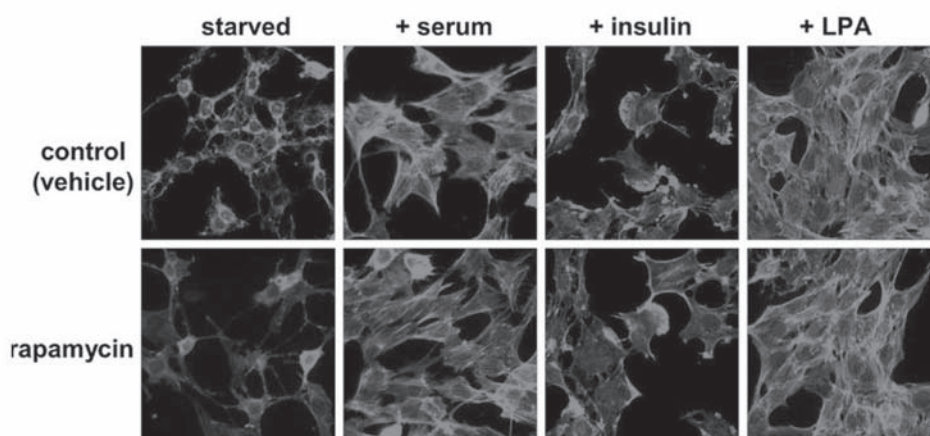


**Figure S1** Serum, insulin or LPA induced actin polymerization is rapamycin insensitive. Drug vehicle (PBS/.0018%EtOH/.0002%Tween20) or rapamycin (20 nM) was added to NIH 3T3 cells 10 minutes prior to stimulation with

serum (10X, 10 min), insulin (1  $\mu$ g/mL, 30 min) or LPA stimulation (3 $\mu$ M, 15 min). Identical results were obtained when 200 nM rapamycin was used.

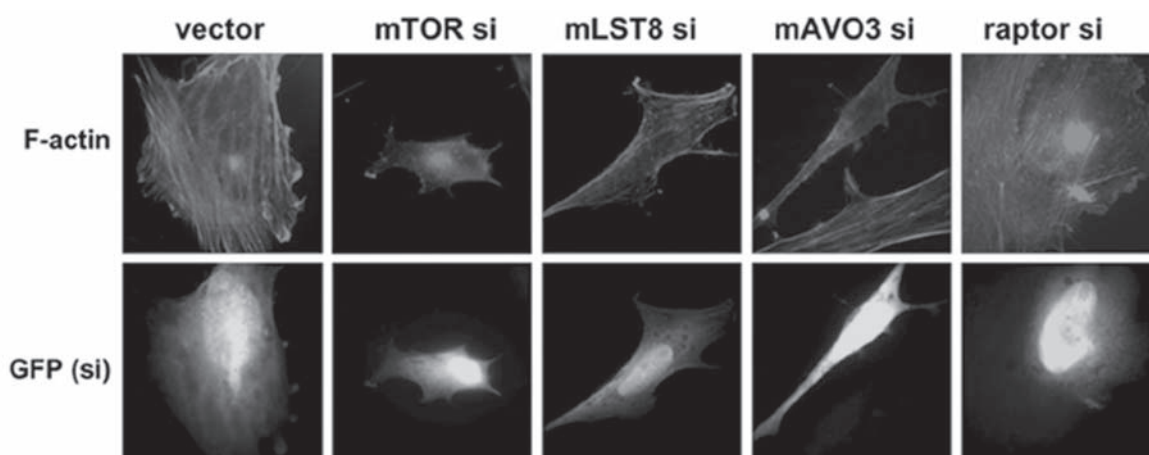


**Figure S2** mTOR, mLST8, and mAVO3, but not raptor are involved in cell spreading, the assembly of F-actin fibers. NIH 3T3 cells were transfected with siRNA for mTOR, mLST8, mAVO3 and raptor and grown in complete

media for 48 hours before harvest (unstarved condition). F-actin was stained using rhodamine-phalloidin. siRNA-transfected cells were detected by GFP fluorescence.



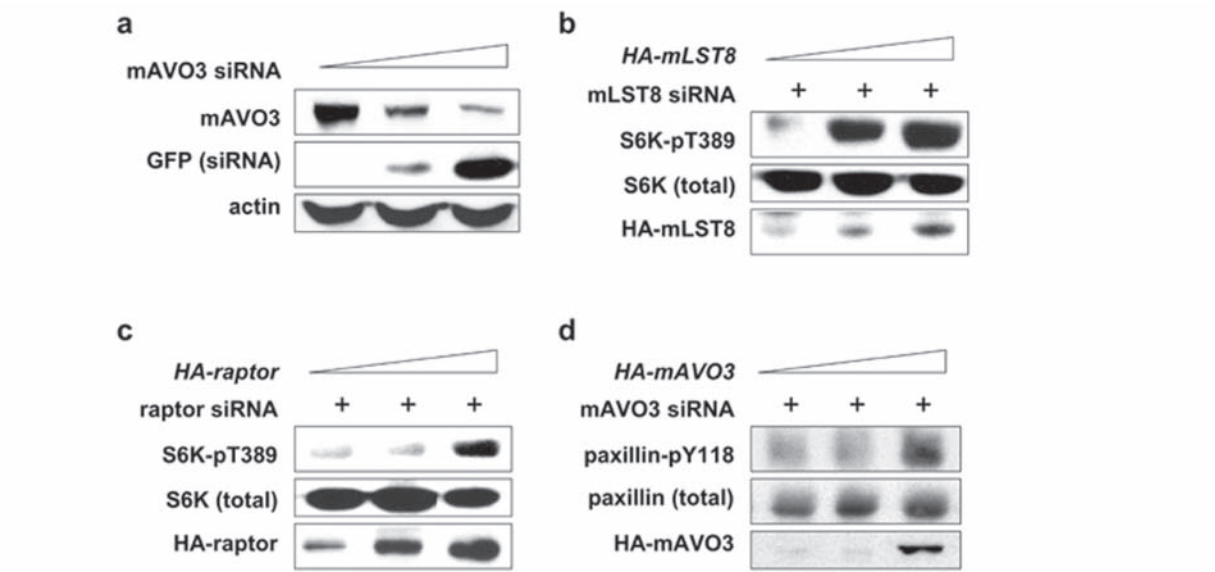


**Figure S3** siRNA constructs reduce expression of targeted proteins. **a.** Endogenous mAVO3 expression is reduced by mAVO3 siRNA. HEK293 cells were transfected with increasing amounts of pSUPER-GFP siRNA against mAVO3 (0, 0.1, 1 µg), and grown in complete media for 48 hours before harvest. mAVO3 was detected using anti-mAVO3 (15T) antibody. The presence of siRNA was detected using GFP antibody. **b.** Overexpression of mLST8 suppresses the effect of mLST8 siRNA. NIH3T3 cells were co-transfected with pSUPER-GFP siRNA against mouse mLST8 and with

increasing amounts of pCI-HA-mLST8 (human). **c.** Overexpression of raptor suppresses the effect of raptor siRNA. NIH 3T3 cells were co-transfected with pSUPER-GFP siRNA against mouse raptor and with increasing amounts of pRK5-HA-raptor (human). **d.** Overexpression of mAVO3 suppresses the effect of mAVO3 siRNA. HEK293 cells were co-transfected with pSUPER-GFP siRNA against mAVO3 and with increasing amounts of pCI-HA-mAVO3. Cells were grown and harvested as above.

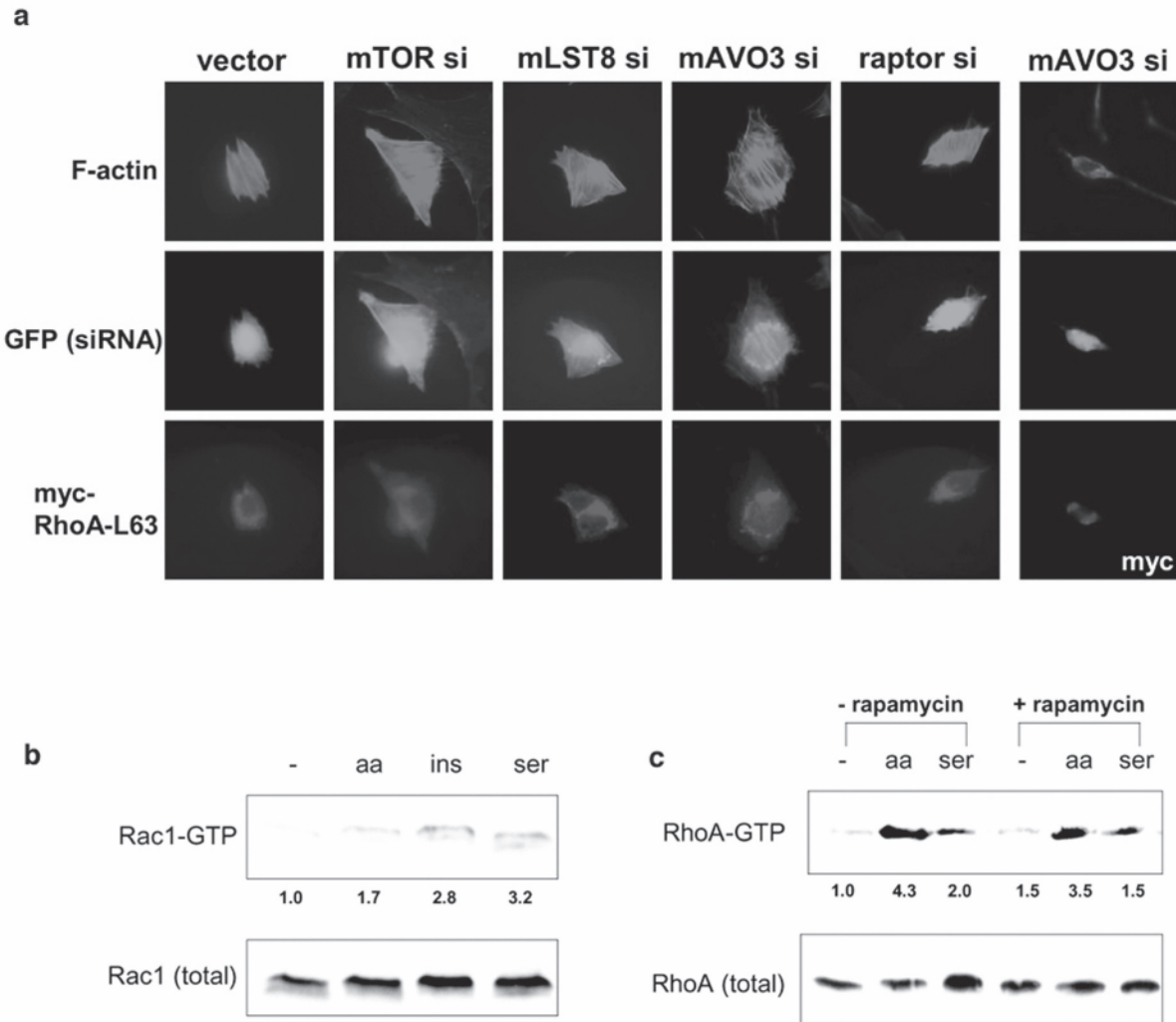


**Figure S4** Rho-type GTPases respond to mTORC2 and nutrients. **a.** Active Rho induces stress fiber formation in mTOR-, mLST8- and mAVO3-knocked down cells. NIH 3T3 cells were co-transfected with 0.5  $\mu$ g myc-RhoA-L63 or myc plasmid (negative control, rightmost column) and 1  $\mu$ g of either vector control, mTOR-, mLST8-, mAVO3- or raptor-siRNA, then starved and processed as in Fig. 5a. **b.** Amino acids activate Rac1. Serum and amino acid-starved NIH 3T3 cells were stimulated with either amino acids (aa; 30 min), insulin (ins; 1  $\mu$ g/mL, 15 min), or serum (ser; 10X, 15 min). Rac1-GTP and total cellular Rac1 were detected as described in Fig. 5. **c.** Amino acids

activate RhoA in a rapamycin insensitive manner. HeLa cells were starved of serum (16 hrs) and amino acids (2 hrs), then pretreated with either drug vehicle or rapamycin (20 nM, 10 min), followed by addition of either amino acids (aa) or serum (ser) for 5 min. RhoA-GTP bound to GST-Rhotekin (RBD) and total cellular RhoA were detected by immunoblot using anti-RhoA. Relative RhoA activity (1.0, 4.3, 2.0, 1.5, 3.5 and 1.5) was determined by comparing the amount of RhoA-GTP bound to GST-Rhotekin (RBD) beads versus total amount of cellular RhoA.